The Journal of Chemical Physics

Vibration-mediated resonant charge separation across the donor–acceptor interface in an organic photovoltaic device

Cite as: J. Chem. Phys. **154**, 154703 (2021); https://doi.org/10.1063/5.0049176
Submitted: 02 March 2021 . Accepted: 06 April 2021 . Published Online: 16 April 2021

Ziyang Hu, Ziyao Xu, and GuanHua Chen

The Journal of Chemical Physics ARTICLE scitation.org/journal/jcp

Vibration-mediated resonant charge separation across the donor–acceptor interface in an organic photovoltaic device

Cite as: J. Chem. Phys. 154, 154703 (2021); doi: 10.1063/5.0049176
Submitted: 2 March 2021 • Accepted: 6 April 2021 •
Published Online: 16 April 2021

Ziyang Hu, Ziyao Xu, and GuanHua Chen[a)]

AFFILIATIONS

Department of Chemistry, The University of Hong Kong, Pokfulam Road, Hong Kong, China

[a)]Author to whom correspondence should be addressed: ghc@everest.hku.hk

ABSTRACT

Examination of a recent open-system Ehrenfest dynamics simulation suggests that a vibration-mediate resonance may play a pivotal role in the charge transfer across a donor–acceptor interface in an organic solar cell. Based on this, a concise dissipative two-level electronic system coupled to a molecular vibrational mode is proposed and solved quantum mechanically. It is found that the charge transfer is enhanced substantially when the vibrational energy quanta is equal to the electronic energy loss across the interface. This vibration-mediate resonant charge transfer process is ultrafast, occurring within 100 fs, comparable to experimental findings. The open-system Ehrenfest dynamics simulation of the two-level model is carried out, and similar results are obtained, which confirms further that the earlier open-system Ehrenfest dynamics simulation indeed correctly predicted the occurrence of the resonant charge transfer across the donor–acceptor interface.

Recently, the vibronic coupling was found to play an important role in charge transfer across the donor–acceptor interface in organic optoelectronics.[1–11] Friend and co-workers reported the dissociation of photo-generated electron–hole pairs across a donor–acceptor interface within 100 fs.[12] Two-dimensional electronic spectroscopy studies have demonstrated the coherence charge transfer across the interface that is driven by an interplay between electronic and vibrational degrees of freedom (in particular, C=C stretching modes).[1,13] Model calculations imply that a combination of several low-frequency vibrational modes and a high-frequency stretching mode can induce vibronic tuned resonant charge transfer.[14,15] We carried out a Ehrenfest molecular dynamics calculation combined with the time-dependent density functional based tight binding for the open-system method (TDDFTB-OS) to simulate that ultrafast charge transfer process across a poly-3-hexylthiophene (P3HT)/[6,6]-phenyl-C_{60} butyric acid methyl ester (PCBM) interface and found that the transfer is coupled coherently to a ≈0.2 eV vibrational mode of P3HT via a strong electron-vibrational coupling at the interface.[16] Figure 1B of Ref. 16 shows the local density of states (LDOS) along the axis perpendicular to the P3HT/PCBM interface and that when a photon is absorbed, an electron is promoted to the LUMO of P3HT from its HOMO, leaving a hole at the HOMO and an electron at the LUMO. When the electron–hole pair arrives at the interface, the electron transfers to the PCBM's LUMO+1 within 100 fs.[16]

We re-examine the results of our work[16] and find surprisingly that the energy difference between the P3HT's LUMO and PCBM's LUMO+1 is 0.2 eV, which is near the vibrational energy quantum $\hbar\omega_v$ of a P3HT's breathing mode (i.e., 201.8 meV), and the breathing mode is precisely the mode that couples vibronically to the electron transfer across the P3HT/PCBM interface in Ref. 16. A close look at the electronic orbitals near the P3HT/PCBM interface shows that P3HT's LUMO, PCBM's LUMO+1, and P3HT's breathing mode are involved in the electron transfer from P3HT to PCBM, while other electronic orbitals and vibrational modes are energetically distanced from the transfer process, as shown in Fig. 1B of Ref. 16. This breathing mode is excited simultaneously as the electron transferred, while other modes, including the low-frequency modes, stay unexcited. This new finding strongly suggests that the direct resonance between one specific high-frequency mode and the electron energy loss may play a key role in the charge separation at the donor–acceptor interface in organic optoelectronic devices.

Perturbative approaches such as Marcus theory and the more general Fermi golden rule give out a fairly good description of resonant electron transfer within the weak electronic hopping regime.[17] The natural questions are (1) whether the resonant charge separation across the interface in the organic optoelectronic device is physical and quantum mechanically correct in the strong electron-vibrational coupling regime and (2) whether open-system Ehrenfest dynamics is adequate to qualitatively capture such quantum mechanical processes as the resonant charge transfer. To answer these questions, we set up a concise model system that captures the physics of the charge separation across the P3HT/PCBM interface and mimics the electronic orbitals and vibrational mode involved in the process.

We design a two-level electronic system coupled to a vibrational mode, as shown in Fig. 1. The solid line with a higher energy represents the donor's molecular orbital (MO), while the lower one represents that of acceptor's MO. The electronic hopping is set to be a constant. The vibrational energy is tunable. Denote two MOs as α (acceptor) and δ (donor), with corresponding creation/annihilation operator as $a_j^\dagger / a_j$, where $j = \alpha, \delta$. The electronic Hamiltonian is

$$H_e = \sum_j \epsilon_j a_j^\dagger a_j + \left(\beta a_\alpha^\dagger a_\delta + \text{h.c.}\right), \tag{1}$$

where $\epsilon_\delta = d$ is the energy of donor's MO and $\epsilon_\alpha = 0$ is the energy of acceptor's MO, β is the hopping amplitude between donor δ and acceptor α, and h.c. stands for the Hermitian conjugate. Considering one vibrational mode in the donor molecule[18] with energy quantum $\hbar\omega_v$, its Hamiltonian can be expressed in terms of corresponding creation and annihilation operators as

$$H_n = \hbar\omega_v\left(a_v^\dagger a_v + 1/2\right). \tag{2}$$

The number operator of this mode is $n_v = a_v^\dagger a_v$. The linear-coupled electron-vibrational interaction Hamiltonian is

$$H_{int} = g_\delta a_\delta^\dagger a_\delta x. \tag{3}$$

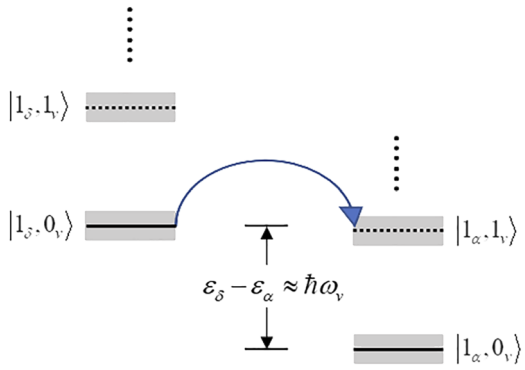

FIG. 1. The diagram showing the energy levels of the coupled electron-vibration states $|n_e, n_v\rangle$ at a donor–acceptor interface. n_e is the occupation number of electrons in either donor's (n_δ) or acceptor's (n_α) molecular orbitals and n_v is the occupation number of the vibrational mode. The shadow on the levels represents energy broadening caused by system–bath coupling and electron-vibrational coupling. Solid lines mean vibrational ground states, and dashed lines mean vibrational excited states $n_v = 1$. The arrow represents charge transfer from donor's $|1_\delta, 0_v\rangle$ to acceptor's $|0_\alpha, 1_v\rangle$.

Here, $x = (2m\omega_v)^{-1}\left(a_v^\dagger + a_v\right)$ is the normal coordinate with m being the reduced mass of this mode. g_δ is the donor's electron–nuclei coupling coefficient. The total Hamiltonian is

$$H = H_e + H_n + H_{int}. \tag{4}$$

To account for the dissipation of electrons to the surrounding environment, a Lindblad master equation is implemented,[19,20]

$$\begin{aligned} i\dot{\sigma} &= [H, \sigma] + i\sum_j Q_j, \\ Q_j &= \gamma_j^+\left(a_j^\dagger \sigma a_j - \frac{1}{2}\left\{a_j a_j^\dagger, \sigma\right\}\right) + \gamma_j^-\left(a_j \sigma a_j^\dagger - \frac{1}{2}\left\{a_j^\dagger a_j, \sigma\right\}\right), \end{aligned} \tag{5}$$

where σ is the total density matrix in space $\mathcal{H}_e \otimes \mathcal{H}_n$, $j = \alpha, \delta$, and $\{A, B\} = AB + BA$. $\gamma_j^+ = \gamma_j N_j$ and $\gamma_j^- = \gamma_j(1 - N_j)$, with γ_j being the dissipation rate and $N_j = \{\exp[(\epsilon_j - \mu_j)/k_B T] + 1\}^{-1}$ being the thermal equilibrium electron numbers. μ_j is the chemical potential of the bulk donor or acceptor. Parameters γ_j describe the effective dissipations through all channels. Since the vibration persists beyond multiple picoseconds, which is much slower than the charge transfer across the donor–acceptor interface,[16,21] we neglect the vibrational dissipation up to the simulation period. The charge transferred from the donor to the acceptor can be calculated as the sum of the acceptor site occupation and the electron dissipated from the acceptor site,

$$q_T(t) = \left\langle 1_\alpha \middle| \text{tr}_{\delta,v}\left[\sigma(t) - \int_0^t d\tau Q_\alpha(\tau)\right] \middle| 1_\alpha \right\rangle. \tag{6}$$

To imitate the energetics of the P3HT/PCBM interface, as shown in Fig. 1B of Ref. 16, we set the electronic energy gap ϵ_δ to 198 meV and Fermi energy $\mu_\alpha = \mu_\delta$ to −1 eV. The dissipation rates are set to $\gamma_\alpha = 18$ meV and $\gamma_\delta = 12$ meV. Due to the large distance (≈3 Å) between donor and acceptor molecules, the electronic hopping β calculated from the P3HT/PCBM structure[16] is 30 meV, which is near the weak electronic coupling regime. Several works reported that the C=C stretching mode of the donor molecules is coupled to the charge transfer,[1,16,22–28] whose reduced mass m is around 6 a.u. from atomistic force calculations. The electron-vibrational coupling coefficient estimated from atomistic calculations based on our previous system is taken to be $g_\delta = -0.41$ eV/bohr, corresponding to the electron-vibrational coupling strength $(2m\omega_v)^{-1}|g_\alpha|$ of 32 meV near resonance. This coupling strength is representative for high energy intra-molecular vibrational modes.[29–31] All simulations are performed in room temperature, $T = 298$ K.

To study the charge transfer process, we start with a mixed state, i.e., one electron occupying donor's MO and the occupation number of the vibrational mode $\langle n_v \rangle$ following Bose–Einstein statistics at temperature $T = 298$ K. The system evolves for 200 fs, as described by Eq. (5). In our calculation, the occupation number of the vibrational mode is limited from zero to two, i.e., $n_v = 0, 1, 2$. For $n_v = 3$ or more, the energy is too high compared to the thermal energy at room temperature, and thus, there is no need to include them in the present calculation, as shown below. Dynamics of charge transfer from the donor to the acceptor is simulated with $\hbar\omega_v$ ranging from 0.14 eV to 0.26 eV. Figure 2 depicts the evolution of donor occupation, transferred charge q_T, and change in $\langle n_v \rangle$ (i.e., $\langle n_v \rangle - \langle n_v \rangle_{t=0}$) for $\hbar\omega_v = 0.20$ eV. The donor occupation (blue dashed line) decreases from 1 to 0 within 200 fs, representing an ultrafast charge transfer process. The decrease in the donor occupation equals

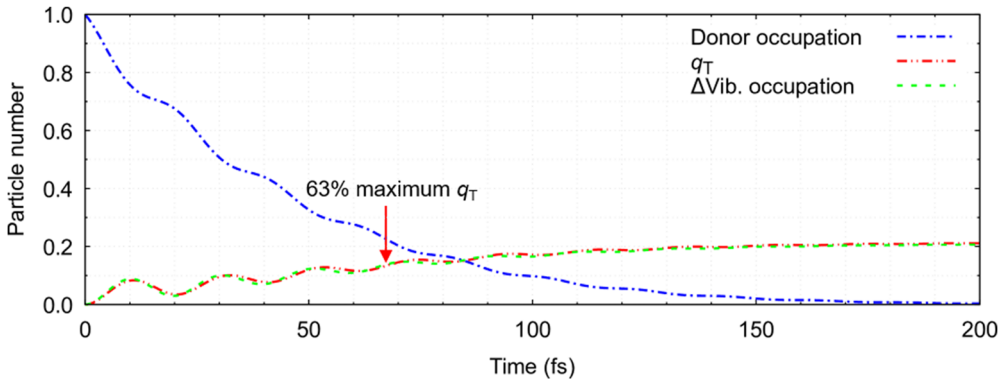

FIG. 2. Evolution of $\left\langle a_\delta^\dagger a_\delta \right\rangle$, q_T, and $\langle n_v \rangle - \langle n_v \rangle_{t=0}$ for quantum dynamics in vibrational space with zero, one, and two occupation numbers. $\hbar\omega_v$ is set to 0.20 eV. The blue, red, and green lines indicate $\left\langle a_\delta^\dagger a_\delta \right\rangle$, q_T, and $\langle n_v \rangle - \langle n_v \rangle_{t=0}$, respectively.

the sum of q_T and the number of electrons carried out of the simulation region by the electron–hole pairs via the donor molecules. It is clear that $\langle n_v \rangle - \langle n_v \rangle_{t=0}$ (green dashed line) overlaps with q_T (red dashed line), signifying the energy transfer from the electron to nuclear vibration accompanied with one phonon excited and one electron transferred simultaneously. The oscillatory behavior of the curves is a signature of the vibronic coupling,[2,4,23,32] and the oscillation frequency is near the vibrational frequency ω_v. We define the charge transfer time as the time when q_T reaches $1 - 1/e$ (≈63%) of its maximum. The charge transfer magnitude and transfer time with different $\hbar\omega_v$ are plotted in Figs. 3(a) and 3(b). The maximum charge transfer magnitude (0.21 electrons) is observed at $\hbar\omega_v = 0.20$ eV, which is the same as the electronic energy gap 0.20 eV. In the meantime, 0.79 electrons are carried away by the electron–hole pairs to the left electrode on the donor side. Resonant charge separation across the interface is thus verified. The resonant transfer time is 67 fs, within 100 fs. The broadening of the transfer magnitude and time with respect to the vibrational energy is caused by the electronic bandwidth and electron–nuclei coupling. These ultrafast dynamics are comparable to the experimental results where charge separation completes within 100 fs.[12]

The C=C breathing mode has a vibrational energy $\hbar\omega_v \approx 0.20$ eV,[16] which is much higher than the thermal energy at room temperature. To examine whether the inclusion up to the second vibrational excited state (i.e., including $|0_v\rangle$, $|1_v\rangle$, and $|2_v\rangle$ in the calculation) is sufficient, we repeat our calculations by including up to the third excited vibrational state $|3_v\rangle$. As shown in Fig. 3, the transfer magnitude for the ground and first excited states (red line) deviates from those with other two cases, while the result for the ground, first, and second excited states overlaps with that of the ground, first, second, and third excited states. This implies that inclusion of the ground, first, and second excited states of the breathing mode is sufficient at room temperature, which confirms the choice we made above.

In the atomistic simulation of large molecular systems, full quantum treatment of nuclear vibrations with large vibrational space is computationally inaccessible. Ehrenfest dynamics is a widely used method for charge transfer simulations.[33,34] The original Ehrenfest dynamics lacks the ability to describe multiple nuclear wave packets moving on separate potential surfaces and suffers from overcoherence and the violation of detailed balance.[35–37] However, multi-configurational Ehrenfest approaches proposed in recent years can correct these failures.[33,34,38,39] Although Ehrenfest dynamics is known for its deficiencies for isolated systems, its applicability has not been well studied for open quantum systems. In our TDDFTB-OS formalism,[40] the wave function of the entire electronic system that includes the system of interests and the environment is modeled by a single Slater determinant or single configuration,[41,42]

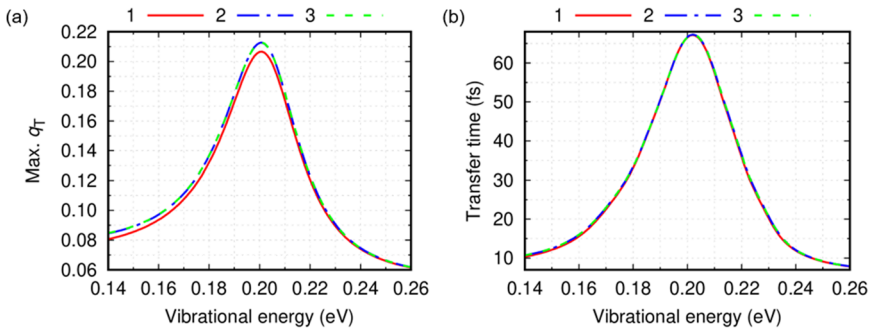

FIG. 3. Charge transfer magnitude and time at different vibrational energies for quantum dynamics. (a) Maximum charge transfer magnitude and (b) transfer time vs vibrational energy. The red solid line indicates the vibrational space with the ground and first excited states, the blue dashed line indicates the ground, first, and second excited states, and the green dashed line indicates the ground, first, second, and third excited states.

and thus, the wave function of the reduced systems, i.e., the system of interests, cannot be represented by a single Slater determinant and is of multi-configuration. Our previous results show that the open-system Ehrenfest dynamics produces qualitatively comparable results with the full quantum method where nuclear vibrations are treated as phonons.[43] In Ref. 16, open-system Ehrenfest dynamics was employed to simulate the charge transfer across the P3HT/PCBM interface. However, it is not clear whether open-system Ehrenfest dynamics has the capability to account for such a quantum process as the resonant charge transfer and whether the resonance suggested from the further analysis of the results in Ref. 16 is physical. To answer these, we carry out an open-system Ehrenfest dynamics simulation of the above two-level model [i.e., two electronic levels coupled to one vibrational mode, cf. Eqs. (1)–(5)] and compare the results to the quantum mechanical results above. The nuclear equation of motion now becomes[44,45]

$$-m\ddot{x} = \mathrm{tr}(\sigma\partial_x H) + m\omega_\nu^2 x, \tag{7}$$

where $\sigma = \sigma_e$ and $H = H_e + H_{int}$ in Eqs. (5)–(7). For Ehrenfest dynamics, the partial trace shall be performed solely over δ in Eq. (6).

Same parameters as above are used to propagate Eqs. (5) and (7). Ehrenfest dynamics is also calculated with $\hbar\omega_\nu$ ranging from 0.14 to 0.26 eV. The initial conditions are sampled according to Boltzmann distribution at 298 K. Figure 4(a) depicts the evolution of donor occupation, q_T, and the change in the vibrational occupation number at $\hbar\omega_\nu = 0.20$ eV with 1000 samples. The vibrational occupation number $\langle n_\nu\rangle$ can be evaluated as $m\left(v^2 + \omega_\nu^2 x^2\right)(2\omega_\nu)^{-1}$. The change in the vibrational occupation number can also be expressed as $-\int \mathrm{d}t\dot{x}\,\mathrm{tr}(\sigma\partial_x H)\omega_\nu^{-1}$ and is thus directly related to the electron-vibrational coupling coefficient g_δ. The charge transfer magnitude and transfer time at different $\hbar\omega_\nu$ with 400 samples for each point are plotted in Figs. 4(b) and 4(c), respectively. The shaded area stands for the standard deviation calculated from the ensemble. At the resonant vibrational energy of 0.20 eV, about 0.12 electrons are transferred within 50 fs. Compared to full quantum dynamics, open-system Ehrenfest dynamics produces qualitatively correct resonant charge transfer with similar transfer magnitude and time. We thus verified the validity of Ehrenfest dynamics for open quantum systems via the simplified model. For comparison, we plot the resonant transfer magnitude and time of the electrons across the P3HT/PCBM interface from the atomistic open-system Ehrenfest dynamics simulation, as reported in Ref. 16 [see the black solid line in Fig. 4(a)], and it is clear that the two Ehrenfest dynamics simulations (atomistic Ehrenfest dynamics and two-level model) are in good agreement. Agreement among the two Ehrenfest dynamics and the above quantum mechanical simulations confirms that the vibration-mediated resonance indeed plays a pivotal role in the charge separation across the interface between P3HT and PCBM and suggests that it may be a general charge transfer mechanism to efficiently separate the electron and hole and lead to the emergence of photocurrent in organic optoelectronics.

We then modulate the environmental dissipation rates, the electronic hopping, and the electron-vibrational coupling for quantum dynamics. The resonant vibrational energy, maximum charge transfer magnitude, and transfer time are inspected in Fig. 5. In Fig. 5(a), it is demonstrated that the dissipation rates have minimum effect on the resonant vibrational energy, whereas in Fig. 5(d), large electronic hopping and small electron-vibrational coupling result in higher resonant vibrational energy since the energy difference between the electron-vibrational states $|0_\alpha 1_\delta 0_\nu\rangle$ and $|1_\alpha 0_\delta 0_\nu\rangle$ is larger in these conditions. In Fig. 5(b), stronger dissipation on the donor site will attenuate the transfer magnitude while it is almost independent of the dissipation on the acceptor site. Both stronger electronic hopping and electron-vibrational coupling intensify the

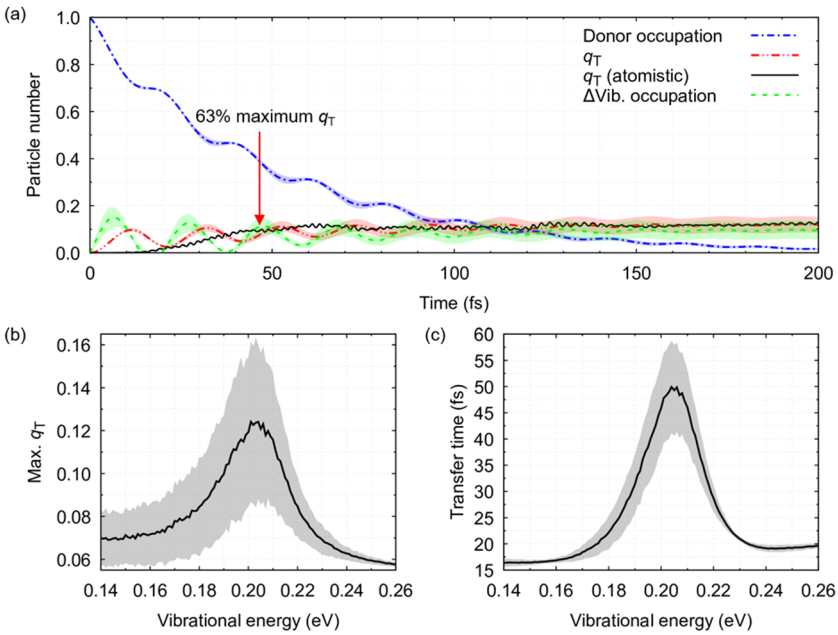

FIG. 4. Simulation results for semiclassical Ehrenfest dynamics. (a) Evolution of $\left\langle a_\delta^\dagger a_\delta\right\rangle$, q_T, and $\langle n_\nu\rangle - \langle n_\nu\rangle_{t=0}$ of the two-level model. The blue, red, and green lines indicate $\left\langle a_\delta^\dagger a_\delta\right\rangle$, q_T, and $\langle n_\nu\rangle - \langle n_\nu\rangle_{t=0}$, respectively. $\hbar\omega_\nu$ is set to 0.20 eV. The transfer time is defined as the time when q_T reaches 63% of its maximum. q_T from our previous atomistic Ehrenfest molecular dynamics simulation is plotted as the black solid line, where zero time is the central time of the Gaussian pulse applied to atomistic systems. Maximum charge transfer magnitude (b) and transfer time (c) are plotted as a function of vibrational energy. The shaded area stands for the standard deviation calculated from the ensemble.

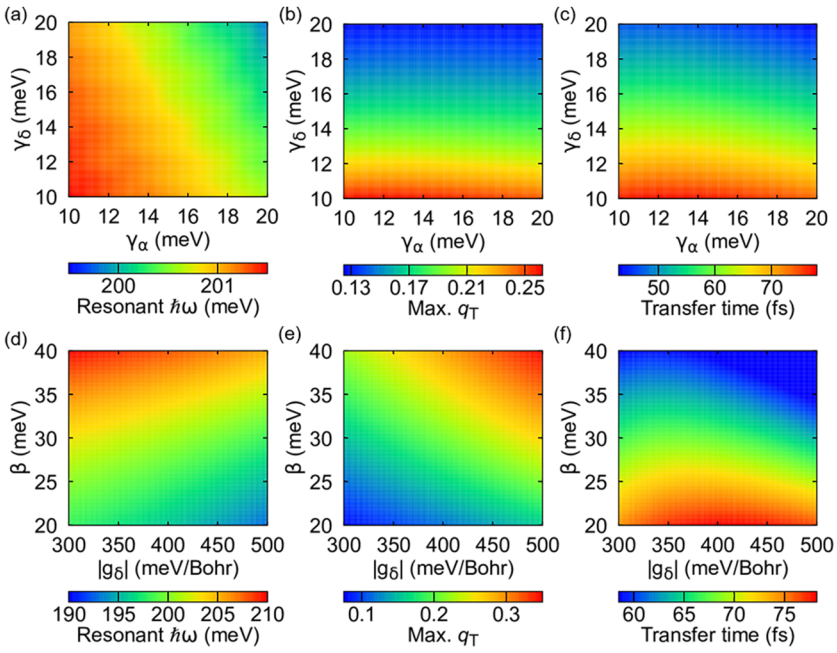

FIG. 5. The dependence of resonant vibrational energy [(a) and (d)], maximum charge transfer magnitude [(b) and (e)], and transfer time [(c) and (f)] on dissipation rates [(a)–(c)], as well as electronic hopping and electron-vibrational coupling [(d)–(f)]. $\beta = 30$ meV and $g_\delta = -0.41$ eV/bohr for panels (a)–(c). $\gamma_\alpha = 18$ meV and $\gamma_\delta = 12$ meV for panels (d)–(f). The resonant vibrational energy is defined as the energy with the largest charge transfer magnitude. (b), (c), (e), and (f) are simulated at the corresponding resonant vibrational energy. All results are calculated by quantum dynamics.

transfer magnitude as expected in Fig. 5(e). The resonant transfer process is always ultrafast under a wide range of dissipation rates and hopping/coupling strength, as shown in Figs. 5(c) and 5(f).

Finally, we alter the vibrational mode to the acceptor site. The resonant charge transfer process still occurs with slightly lower transfer magnitude for both quantum and Ehrenfest dynamics, as depicted in Fig. (6), possibly because the electron resides on the donor site at the beginning phase.

We have checked quantum mechanically that the vibration-mediated resonant charge separation across the interface in the organic optoelectronic device is physical and ultrafast (within 100 fs) by solving a simple two-level dissipative electronic system coupled to a vibrational mode. With the mechanism, this ultrafast phenomenon is expected to exist under a wide range of environmental parameters. This finding confirms the experimental results that one particular high-frequency vibrational mode can be pivotal to the ultrafast charge separation process without the tuning of electronic energy levels by low-frequency modes. We also showed that open-system Ehrenfest dynamics is adequate to qualitatively capture such a resonant charge transfer process, enabling the practical simulation for large scale atomistic systems. In realistic organic solar cells, usually one specific high-frequency mode is strongly coupled to an electronic state, which is actively involved in the charge transfer process. The electronic state is expected to be the frontier orbitals. We can thus tailor the structure to modulate the molecular vibrational frequency of the strongly coupled mode and the electronic energy gap between frontier orbitals. By aligning the energy gap with the vibrational frequencies, the overall quantum efficiencies of organic optoelectronic devices can be optimized. This would be helpful for the design of highly efficient organic solar cells.

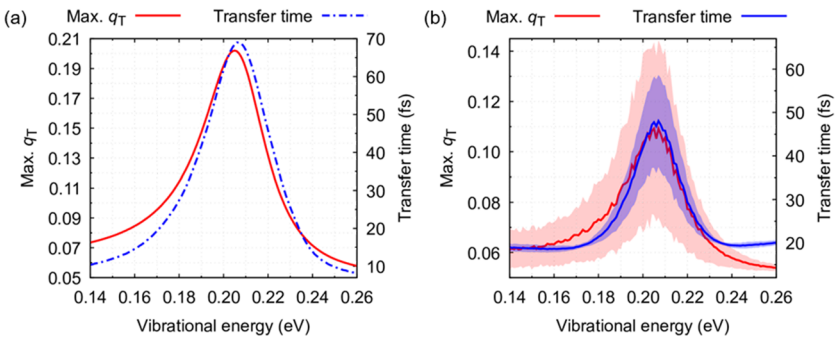

FIG. 6. Maximum charge transfer magnitude and transfer time for quantum dynamics (a) and semi-classical Ehrenfest dynamics (b) with electron-vibrational coupling on the acceptor site. The red line indicates the charge transfer magnitude (left axis), and the blue line indicates the transfer time (right axis). The shaded area stands for the standard deviation calculated from the ensemble.

AUTHORS' CONTRIBUTIONS

Z.H. and Z.X. contributed equally to this work.

This work was supported by the RGC General Research Fund (Grant No. 17309620) and Hong Kong Quantum AI Lab Limited.

The authors declare no competing financial interest.

DATA AVAILABILITY

The data that support the findings of this study are available within the article.

REFERENCES

[1] A. De Sio and C. Lienau, Phys. Chem. Chem. Phys. **19**, 18813–18830 (2017).
[2] H.-G. Duan, P. Nalbach, R. J. D. Miller, and M. Thorwart, J. Phys. Chem. Lett. **10**, 1206–1211 (2019).
[3] J.-L. Brédas, E. H. Sargent, and G. D. Scholes, Nat. Mater. **16**, 35–44 (2017).
[4] V. Tiwari, W. K. Peters, and D. M. Jonas, Proc. Natl. Acad. Sci. U. S. A. **110**, 1203–1208 (2013).
[5] S. Rafiq and G. D. Scholes, J. Am. Chem. Soc. **141**, 708–722 (2019).
[6] W. Popp, M. Polkehn, R. Binder, and I. Burghardt, J. Phys. Chem. Lett. **10**, 3326–3332 (2019).
[7] T. R. Nelson, D. Ondarse-Alvarez, N. Oldani, B. Rodriguez-Hernandez, L. Alfonso-Hernandez, J. F. Galindo, V. D. Kleiman, S. Fernandez-Alberti, A. E. Roitberg, and S. Tretiak, Nat. Commun. **9**, 2316 (2018).
[8] S. M. Falke, C. A. Rozzi, D. Brida, M. Maiuri, M. Amato, E. Sommer, A. De Sio, A. Rubio, G. Cerullo, E. Molinari, and C. Lienau, Science **344**, 1001 (2014).
[9] A. Kelly, Faraday Discuss. **221**, 547–563 (2020).
[10] M. Polkehn, H. Tamura, and I. Burghardt, J. Phys. B: At., Mol. Opt. Phys. **51**, 014003 (2017).
[11] G. Chen and S. Mukamel, J. Am. Chem. Soc. **117**, 4945–4964 (1995).
[12] S. Gélinas, A. Rao, A. Kumar, S. L. Smith, A. W. Chin, J. Clark, T. S. van der Poll, G. C. Bazan, and R. H. Friend, Science **343**, 512 (2014).
[13] A. Mandal, J. D. Schultz, Y.-L. Wu, A. F. Coleman, R. M. Young, and M. R. Wasielewski, J. Phys. Chem. Lett. **10**, 3509–3515 (2019).
[14] H. Tamura, J. Chem. Phys. **130**, 214705 (2009).
[15] H. Tamura, R. Martinazzo, M. Ruckenbauer, and I. Burghardt, J. Chem. Phys. **137**, 22A540 (2012).
[16] Z. Xu, Y. Zhou, L. Groß, A. De Sio, C. Y. Yam, C. Lienau, T. Frauenheim, and G. Chen, Nano Lett. **19**, 8630–8637 (2019).
[17] R. A. Marcus and N. Sutin, Biochim. Biophys. Acta, Rev. Bioenerg. **811**, 265–322 (1985).
[18] M. Cardona and G. Güntherodt, *Light Scattering in Solids VIII: Fullerenes, Semiconductor Surfaces, Coherent Phonons*, Topics in Applied Physics Vol. 76 (Springer, 2000), pp. 1–26.
[19] S. Ajisaka and F. Barra, Phys. Rev. B **87**, 195114 (2013).
[20] J. E. Elenewski, D. Gruss, and M. Zwolak, J. Chem. Phys. **147**, 151101 (2017).
[21] Y. Song, S. N. Clafton, R. D. Pensack, T. W. Kee, and G. D. Scholes, Nat. Commun. **5**, 4933 (2014).
[22] S. Tretiak, A. Saxena, R. L. Martin, and A. R. Bishop, Phys. Rev. Lett. **89**, 097402 (2002).
[23] A. De Sio, F. Troiani, M. Maiuri, J. Réhault, E. Sommer, J. Lim, S. F. Huelga, M. B. Plenio, C. A. Rozzi, G. Cerullo, E. Molinari, and C. Lienau, Nat. Commun. **7**, 13742 (2016).
[24] J. Razzell-Hollis, S. Limbu, and J.-S. Kim, J. Phys. Chem. C **120**, 10806–10814 (2016).
[25] A. De Sio, F. V. d. A. Camargo, K. Winte, E. Sommer, F. Branchi, G. Cerullo, and C. Lienau, Eur. Phys. J. B **91**, 236 (2018).
[26] S. Joseph, M. K. Ravva, and J.-L. Bredas, J. Phys. Chem. Lett. **8**, 5171–5176 (2017).
[27] A. A. Bakulin, R. Lovrincic, X. Yu, O. Selig, H. J. Bakker, Y. L. A. Rezus, P. K. Nayak, A. Fonari, V. Coropceanu, J.-L. Brédas, and D. Cahen, Nat. Commun. **6**, 7880 (2015).
[28] J. Clark, C. Silva, R. H. Friend, and F. C. Spano, Phys. Rev. Lett. **98**, 206406 (2007).
[29] E. J. O'Reilly and A. Olaya-Castro, Nat. Commun. **5**, 3012 (2014).
[30] A. Kolli, E. J. O'Reilly, G. D. Scholes, and A. Olaya-Castro, J. Chem. Phys. **137**, 174109 (2012).
[31] J. M. Womick and A. M. Moran, J. Phys. Chem. B **115**, 1347–1356 (2011).
[32] Y. Yao, X. Xie, and H. Ma, J. Phys. Chem. Lett. **7**, 4830–4835 (2016).
[33] T. Ma, M. Bonfanti, P. Eisenbrandt, R. Martinazzo, and I. Burghardt, J. Chem. Phys. **149**, 244107 (2018).
[34] P. Nijjar, J. Jankowska, and O. V. Prezhdo, J. Chem. Phys. **150**, 204124 (2019).
[35] J. E. Subotnik, J. Chem. Phys. **132**, 134112 (2010).
[36] S. K. Min, F. Agostini, and E. K. U. Gross, Phys. Rev. Lett. **115**, 073001 (2015).
[37] P. V. Parandekar and J. C. Tully, J. Chem. Theory Comput. **2**, 229–235 (2006).
[38] D. V. Makhov, C. Symonds, S. Fernandez-Alberti, and D. V. Shalashilin, Chem. Phys. **493**, 200–218 (2017).
[39] L. Chen, M. F. Gelin, and D. V. Shalashilin, J. Chem. Phys. **151**, 244116 (2019).
[40] H. Xie, F. Jiang, H. Tian, X. Zheng, Y. Kwok, S. Chen, C. Yam, Y. Yan, and G. Chen, J. Chem. Phys. **137**, 044113 (2012).
[41] S. Yokojima and G. Chen, Phys. Rev. B **59**, 7259–7262 (1999).
[42] W. Liang, G. Chen, Z. Li, and Z.-K. Tang, Appl. Phys. Lett. **80**, 3415–3417 (2002).
[43] S. Chen, W. Zhou, Q. Zhang, Y. Kwok, G. Chen, and M. A. Ratner, J. Phys. Chem. Lett. **8**, 5166–5170 (2017).
[44] F. Wang, C. Y. Yam, L. Hu, and G. Chen, J. Chem. Phys. **135**, 044126 (2011).
[45] T. C. Berkelbach, T. E. Markland, and D. R. Reichman, J. Chem. Phys. **136**, 084104 (2012).